BIOLOGY OF REPRODUCTION **78,** 115–126 (2008)
Published online before print 17 October 2007.
DOI 10.1095/biolreprod.107.061366

Proteolytic Activity of the 26S Proteasome Is Required for the Meiotic Resumption, Germinal Vesicle Breakdown, and Cumulus Expansion of Porcine Cumulus-Oocyte Complexes Matured In Vitro[1]

Young-Joo Yi,[3,4] Eva Nagyova,[5] Gaurishankar Manandhar,[3] Radek Procházka,[5] Miriam Sutovsky,[3] Chang-Sik Park,[4] and Peter Sutovsky[2,3,6]

Division of Animal Sciences,[3] University of Missouri-Columbia, Columbia, Missouri 65211
Research Center for Transgenic Cloned Pigs,[4] Chungnam National University, Daejeon, Korea
Institute of Animal Physiology & Genetics,[5] Czech Academy of Sciences, 277 21 Liběchov, Czech Republic
Department of Obstetrics & Gynecology,[6] University of Missouri-Columbia, Columbia, Missouri 65211

ABSTRACT

The resumption of oocyte meiosis in mammals encompasses the landmark event of oocyte germinal vesicle (GV) breakdown (GVBD), accompanied by the modification of cell-to-cell communication and adhesion between the oocyte and surrounding cumulus cells. The concomitant cumulus expansion relies on microfilament-cytoskeletal remodeling and extracellular matrix (ECM) deposition. We hypothesized that this multifaceted remodeling event requires substrate-specific proteolysis by the ubiquitin-proteasome pathway (UPP). We evaluated meiotic progression, cytoskeletal dynamics, and the production of cumulus ECM in porcine cumulus-oocyte complexes (COCs) cultured with or without 10–200 μM MG132, a specific proteasomal inhibitor, for the first 22 h of in vitro maturation, followed by 22 h of culture with or without MG132. Treatment with 10 μM MG132 arrested 28.4% of oocytes in GV stage (vs. 1.3% in control), 43.1% in prometaphase I, and 16.2% in metaphase I, whereas 83.7% of control ova reached metaphase II (0% of MG132 reached metaphase II). The proportion of GV-stage ova increased progressively to >90% with increased concentration of MG132 (20–200 μM). Furthermore, MG132 blocked the extrusion of the first polar body and degradation of F-actin-rich transzonal projections (TZP) interconnecting cumulus cells with the oocyte. The microfilament disruptor cytochalasin E (CE) prevented cumulus expansion but accelerated the breakdown of TZPs. Ova treated with a combination of 10 μM MG132 and 10 μM CE underwent GVBD, despite the inhibition of proteasomal activity. However, 90.0% of cumulus-free ova treated with 10 μM MG132 remained in GV stage, compared with 16.7% GV ova in control. Cumulus expansion, retention of hyaluronic acid, and the deposition of cumulus ECM relying on the covalent transfer of heavy chains of inter-alpha trypsin inhibitor (IαI) were also inhibited by MG132. Cumulus expansion in control COCs was accompanied by the degradation of ubiquitin-C-terminal hydrolase L3, an important regulator of UPP. RAC1, a UPP-controlled regulator of actin polymerization was maintained at steady levels throughout cumulus expansion. We conclude that proteasomal proteolysis has multiple functions in the progression of oocyte meiosis beyond GV and metaphase I stage, polar body extrusion, and cumulus expansion.

cumulus expansion, FSH, germinal vesicle breakdown, LH, MG132, oocyte, oocyte maturation, porcine, proteasome, ubiquitin

INTRODUCTION

Before the preovulatory gonadotropin surge, the mammalian oocytes arrested at the dictyate stage of meiosis I are surrounded by the cumulus oophorus, a specialized population of cumulus-granulosa cells in the antral ovarian follicle. Cumulus oophorus plays important roles in oogenesis, such as keeping the oocyte under meiotic arrest, inducting meiotic resumption, and supporting nuclear and cytoplasmic maturation of the oocyte [1]. The cumulus cells synthesize cAMP, a meiosis inhibitory factor that is the major survival factor in the antral follicle [2]. The resumption of oocyte meiosis is accompanied by the disappearance of the zona pellucida-spanning, actin microfilament-rich transzonal projections (TZPs) connecting the cumulus cells with the oocyte. This event is followed by the alteration of gap junctional communication in the cumulus oophorus, extensive rearrangement of actin microfilaments in the cumulus cells, and deposition of the extracellular matrix (ECM) parallel to cumulus expansion [3, 4]. Consequently, the communication between cumulus cells and the oocyte is altered in an expanded cumulus [5–7]. Metabolic uncoupling within the expanding cumulus-oocyte complexes (COCs) is believed to cause the decline of ooplasmic cAMP levels and lead to activation of CDC2/CDK1 kinase and mitogen-activated protein (MAP) kinase in the oocyte [8]. Subsequently, the surrounding mass of cumulus oophorus starts to expand because of massive hyaluronan synthesis [9] and extensive cytoskeletal rearrangement within the cumulus oophorus [4, 10–12]. The actin-rich TZPs are thought to be retracted and maintain fewer connections with the oocyte after cumulus expansion [13], but the actual mechanism altering the TZPs upon gonadotropin surge is not known.

Cumulus expansion in rodents [14–16] occurs after germinal vesicle breakdown (GVBD), but in the porcine model, partially expanded cumuli are observed prior to GVBD onset [17, 18]. In an in vitro culture system, cumulus expansion

[1]Supported by National Research Initiative (NRI) Competitive Grants #2002-35203-12237 and 2007-35203-18274 from the US Department of Agriculture (USDA) Cooperative State Research, Education, and Extension Service, USDA-NRI Discovery Award 2005, and seed funding from the Food for the 21st Century Program of the University of Missouri-Columbia. Y.-J.Y. and C.-S.P. were supported by grant R11-2002-100-00000-0 from ERC Program of Korea Science & Engineering Foundation (KOSEF). E.N. was supported by award 305/05/0960 from the Grant Agency of the Czech Republic.
[2]Correspondence: Peter Sutovsky, Associate Professor, University of Missouri-Columbia, S141 ASRC, 920 East Campus Dr., Columbia, MO 65211-5300. FAX: 573 884 5540; e-mail: SutovskyP@missouri.edu

Received: 8 March 2007.
First decision: 26 May 2007.
Accepted: 8 October 2007.

ISSN: 0006-3363. http://www.biolreprod.org

and metabolic uncoupling can be induced by FSH [19, 20] as well as by the adenyl-cyclase-activating drug forskolin [18], causing an increase in cAMP concentration in the cumulus cells [6, 15, 20]. Normal cumulus expansion in vitro is conducive to increased maturation rates [21] and higher rates of male pronuclear formation after sperm penetration [22]. Cumulus expansion is the result of interplay between microfilament-cytoskeletal rearrangement and increased synthesis of ECM composed mainly of hyaluronic acid (HA), glycosaminoglycans, and glycoproteins [5, 15, 23–25]. The FSH-induced synthesis of HA can be measured by the incorporation of [^{3}H]-glucosamine into HA either in complexes alone (retained HA) or in medium plus complexes (total HA) [26]. The heavy chains (HCs) of serum derived from inter-alpha trypsin inhibitor (IαI) molecules become covalently linked to HA during mouse cumulus expansion in vivo [27, 28]. The covalent transfer of IαI to HA is catalyzed by the factors synthesized within the ovarian follicle [29–31]. The molecules of IαI can freely cross the blood-follicle barrier. Consequently, follicular fluid collected at any stage of folliculogenesis can be used to replace serum during porcine oocyte maturation in vitro [32].

Ubiquitin is a highly conserved protein of 76 amino acid residues that binds covalently in a tandem fashion to substrate proteins through a multistep enzymatic pathway [33]. The resultant polyubiquitin chain-tagged substrates are recognized by the 26S proteasome, a multicatalytic, substrate-specific protease composed of the barrel-shaped 20S proteasomal proteolytic core capped with one or two 19S regulatory complexes [34]. After the 19S regulatory complex removes the polyubiquitin chain, the substrate protein is translocated to 20S proteasomal core, where it is degraded into small peptides [35]. The rate of proteasomal proteolysis is controlled by deubiquitinating enzymes, including the ubiquitin-C-terminal hydrolases (UCHs) and ubiquitin-specific proteases [36]. Several groups reported the role of the ubiquitin-proteasome pathway (UPP) in the invertebrate oocyte maturation. Cyclins, CDK-inhibitor proteins, and *c-Mos* gene product are ubiquitinated and degraded by the 26S proteasome during the M phase of the cell cycle [37]. Takagi Sawada et al. [38] blocked starfish oocyte maturation by the addition of MG115, a specific proteasomal inhibitor, and proposed that the proteasomal activity triggers the activation of pre-MPF through the dephosphorylation of CDC2 kinase in response to the hormonal stimulus. Recently, the metaphase-anaphase transition was blocked effectively by MG132, a highly specific and reversible proteasomal inhibitor, during oocyte maturation in several mammalian species [39–42]. The inhibition of metaphase-anaphase transition by MG132 is consistent with the requirement of proteasomal activity for cyclin degradation at this stage of the cell cycle [43]. The present study has examined the effect of MG132 on early (GVBD) and late events (cytokinesis/polar body extrusion) of oocyte meiotic maturation and cumulus expansion of porcine COCs, and it investigated the interplay between proteasomal activities, microfilament dynamics, and ECM synthesis during in vitro maturation (IVM).

MATERIALS AND METHODS

Collection and IVM of Porcine Oocytes

Ovaries were collected from prepubertal gilts at a local slaughterhouse and transported to the laboratory in a warm box (25°C–30°C). Cumulus-oocyte complexes were aspirated from antral follicles (3–6 mm in diameter) using an 18-gauge needle attached to a 10-ml disposable syringe. The COCs were washed three times in HEPES-buffered Tyrode lactate (TL-HEPES-PVA) medium containing 0.1% (w/v) polyvinyl alcohol (PVA) and three times with the maturation medium [44]. A total of 50 COCs were transferred to 500 μl of the maturation medium that had been covered with mineral oil in a four-well multidish (Nunc, Roskilde, Denmark) and equilibrated at 38.5°C, 5% CO_2 in air. The medium used for oocyte maturation was tissue culture medium 199 (TCM199; Gibco, Grand Island, NY) supplemented with 0.1% PVA, 3.05 mM D-glucose, 0.91 mM sodium pyruvate, 0.57 mM cysteine, 0.5 μg/ml LH (L 5269; Sigma), 0.5 μg/ml FSH (F 2293; Sigma), 10 ng/ml epidermal growth factor (E 4127; Sigma), 10% porcine follicular fluid, 75 μg/ml penicillin G, and 50 μg/ml streptomycin sulfate. After 22 h of culture, oocytes were cultured without LH and FSH for 22 h at 38.5°C, 5% CO_2 in the air. Reversible proteasomal inhibitor MG132 (Biomol Research Laboratories Inc., Plymouth Meeting, PA) was dissolved in ethanol to prepare the stock solution. All chemicals, including MG132 and cytochalasin E (CE), were added to IVM medium at the time of oocyte addition immediately prior to IVM.

Unless otherwise mentioned, all chemicals used in this study were purchased from Sigma Chemical Co. (St. Louis, MO).

Immunofluorescence and Epifluorescence Microscopy

Intact cumulus cell-enclosed oocytes and cumulus cell-free oocytes were fixed before IVM or after 44 h of IVM. To remove cumulus cells, oocytes were incubated with 0.1% hyaluronidase in TL-HEPES-PVA medium and were washed three times with TL-HEPES-PVA medium. Oocytes were transferred into the first well of a nine-well Pyrex brand glass plate (Fisher Scientific, Brightwaters, NY) filled with 400 μl of 37°C warm PBS, and 100 μl of 10% formaldehyde was slowly added to bring the final concentration of formaldehyde to 2% [45]. After 40 min of fixation at room temperature, oocytes were washed in two wells of PBS, fixative was removed, and the plates were wrapped in Handi-Wrap plastic wrap and stored for 1–7 days at 4°C. Prior to fluorescence processing, oocytes were permeabilized in PBS with 0.1% Triton X-100 at room temperature for 40 min. Samples were incubated with Alexa Fluor 488-phalloidin (1:50 dilution; Molecular Probes, Eugene, OR) and 2.5 μg/ml 4′,6′-diamidino-2-phenylindole (DAPI; Molecular Probes) or 10 μg/ml propidium iodide (PI; DNA stains; Sigma) for 40 min to observe microfilament organizations.

To examine configurations of nuclear envelope and proteasomes at the germinal vesicle (GV) and GVBD stages of oocyte maturation, the formaldehyde-fixed oocytes were blocked for 25 min in 0.1 M PBS containing 5% normal goat serum and 0.1% Triton X-100 after permeabilization. Oocytes were incubated for 40 min with mAb 414, a mouse immunoglobulin G (IgG) against nuclear pore complex (1:200 dilution; BabCo/Covance, Berkeley, CA) and a rabbit polyclonal antibody against 20S proteasomal core recognizing multiple α-type and β-type core subunits (1:200 dilution; Biomol). After washing, oocytes were incubated for 40 min with goat-anti-mouse (GAM)-IgG-fluorescein isothiocyanate to detect mAb 414, and goat-anti-rabbit (GAR)-TRITC to detect anti-20S proteasome α/β subunit antibody (1:80 dilutions, respectively; Zymed Inc., San Francisco, CA). DNA was stained with DAPI (2.5 μg/ml). Image acquisition was performed using a Nikon Eclipse 800 microscope (Nikon Instruments Inc., Melville, NY) with a Cool Snap camera (Roper Scientific, Tucson, AZ) and MetaMorph software (Universal Imaging Corp., Downingtown, PA) and an Olympus Fluoview confocal laser scanning microscope. Data were archived on CD-R compact discs and edited using Adobe Photoshop 7.0 (Adobe Systems, Mountain View, CA).

Western Blotting

Groups of 30 COCs isolated before (0 h) or after (22 h) in vitro culture in the presence of FSH/LH in medium with or without 100 μM MG132 were prepared for Western blot analysis by a procedure described previously [32]. Control in vivo COCs were obtained as described [32]. Shortly, COCs were washed in PBS containing a cocktail of protease inhibitors (PBS-PI) (Complete Mini; Boehringer Mannheim, Mannheim, Germany) and digested with 1 IU *Streptomyces* hyaluronidase (Merck-Calbiochem, Prague, Czech Republic) at 37°C for 1 h. The digested samples were centrifuged at 300 × *g* for 7 min to separate the matrix extract from the cell pellet. Reducing Laemmli buffer then was added to each fraction, and all samples were boiled at 99°C for 4 min, separated in 7.5% acrylamide/SDS gels, and transferred to Hypobond-P membranes (Amersham-Pharmacia, Prague, Czech Republic). Membranes were blocked with 5% nonfat dry milk in Tris-buffer solution (TBS) for 2 h at room temperature. Primary and secondary antibodies were diluted in TBS containing 5% BSA and 0.05% Tween 20. After electrophoresis, the proteins were detected with rabbit anti-human IαI (1:2000 dilution; DAKO, Carpenteria, CA) and anti-actin/ACTB (1:500 dilution; Sigma-Aldrich, Prague, Czech Republic) antibodies, followed by a horseradish peroxidase-linked F(ab′)$_2$ fragment of the anti-rabbit IgG, as a secondary antibody (1:10 000 dilution; Amersham-Biosciences) for 1 h at room temperature. RAC1 GTPase was

detected using the mouse IgG generated against 21-kDa human RAC1 (Becton Dickinson, BD Transduction Laboratories). Ubiquitin C-terminal hydrolase L3 (UCHL3) was detected by the affinity-purified rabbit serum raised against a synthetic peptide corresponding to a C-terminal domain of human UCHL3 (MBL, Woburn, MA). The protein bands were detected by enhanced chemiluminiscence (Amersham-Pharmacia).

Hyaluronic Acid Synthesis Assay

Groups of 10 COCs were cultured for 23 h in 100 μl culture medium in the presence of FSH/LH and 2.5 μCi of [^{3}H]-glucosamine hydrochloride (MGP, Zlín, Czech Republic) with or without 100 μM MG132. Synthesis of hyaluronic acid (HA) was measured using a procedure described previously [26]. Briefly, the cultures were terminated by adding 10 μl of a solution containing 50 mg/ml pronase (Sigma-Aldrich) and Triton X-100 in 0.2 M Tris buffer pH 7.8. The samples were incubated for 1 h at 38.5°C and then transferred onto Whatman 3MM filter paper circles. The circles were air dried and then washed through three changes of solution containing 0.5% cetylpyridinium chloride and 10 mM nonradioactive glucosamine hydrochloride (Sigma-Aldrich). The circles were dried once again, and radioactivity was measured using a liquid scintillation counter. Synthesis of HA was measured either in medium plus complexes (total HA) or within the complexes alone (retained HA).

Statistical Analysis

Analysis of variance (ANOVA) was performed using the general linear model (GLM) procedure of the Statistical Analysis System (Cary, NC). The Duncan multiple-range test was used to compare mean value of individual treatments. The F-value was considered significant at $P < 0.05$.

RESULTS

MG132 Prevents Gonadotropin-Induced Degradation of TZPs and Cytoskeletal Rearrangements Within Cumulus Oophorus

Confocal microscopy was used to evaluate the TZPs and microfilament distribution at different stages of oocyte maturation with and without proteasomal inhibitors. Immature porcine oocytes were surrounded by a compact mass of round cumulus cells in the freshly isolated COCs. The innermost layer of cumulus/corona radiate cells was connected to oocyte surface through numerous F-actin-rich TZPs (Fig. 1A). Few TZPs remained on the ZP after IVM (Fig. 1B). Addition of 10 μM MG132 in the IVM medium for 44 h prevented cumulus expansion and breakdown of TZPs (Fig. 1C). When the COCs were cultured in the presence of MG132 for 22 h, and then cultured without MG132 for an additional 22 h, TZPs remained lodged in the ZP and connected to oocyte surface (Fig. 1D). However, the extracellular spaces between cumulus cells became enlarged at the periphery of COCs and bundles of filamentous actin (F-actin) typical of early stages of cumulus expansion [11, 12] emerged (Fig. 1D). In the COCs cultured in the absence of MG132 for 22 h and subsequently cultured with MG132 for 22 h, cumulus masses already expanded under the influence of FSH/LH stimulation within the first 22 h of culture, and few TZPs remained embedded in the ZP (Fig. 1E).

MG132 Prevents Cumulus Expansion and Decelerates Meiotic Maturation

Progression of oocyte meiosis was evaluated by conventional light microscopy of oocytes stained with DNA stain DAPI. GV retention was higher in the presence of MG132 for 44 h than it was after MG132 addition into the first or second 22 h of IVM only. Most oocytes became arrested in prometaphase I or metaphase I when COCs were cultured with MG132 for the whole 44 h. In the absence of MG132, 83.7% of ova reached metaphase II after 44 h of IVM (Fig. 2). The extent of cumulus expansion was evaluated under a dissecting microscope at 0, 22, and 44 h of IVM with or without MG132 and showed complete inhibition in the presence of 10 μM MG132 present in the IVM medium for the whole 44-h culture period (Supplemental Data Figure 1 available online at www.biolreprod.org).

Concentration-Dependent Inhibition of GVBD and Metaphase-Anaphase Transition by MG132

Exposure to progressively increasing concentrations of MG132 caused a dose-dependent delay of GVBD and meiosis in the ova from in vitro-matured COCs (Fig. 3A). The rates of ova with intact GV after 44 h of IVM were significantly ($P < 0.05$) higher in the presence of 150 and 200 μM MG132 than in the presence of 20–100 μM MG132. The rates of prometaphase I, metaphase I, anaphase I, telophase I, and metaphase II decreased proportionally with increased concentrations of MG132 (Fig. 3A). The arrest of oocyte meiosis at metaphase-anaphase transition was expected because of the known requirement of proteasomal activity for the degradation of cyclin B at this stage of meiosis. In a concomitantly cultured control group, porcine COCs were cultured with different concentrations of ethanol (a vehicle for MG132; Fig. 3B).

To examine the process of GVBD and accompanying redistribution of proteasomes in the maturing oocytes, COCs cultured in the presence or absence of 10 μM MG132 were fixed and incubated with a mixture of mAb 414, a mouse IgG against nuclear pore complex (NPC; marker of intact nuclear envelope signifying intact GV), and a rabbit polyclonal antibody to 20S proteasomal core recognizing multiple α-type and β-type proteasomal core subunits. Gradual disappearance of NPCs was observed prior to chromosome condensation and prior to the disappearance of proteasomes from the GV during GVBD process in the control oocyte not exposed to MG132 (Fig. 3C, a–d). Both the proteasomes and NPCs were completely absent from metaphase I stage oocytes (Fig. 3C, e). The rate of GV retention in the presence of 100 μM MG132 for 44 h (Fig. 4A) was comparable to that in experiments with 150–200 MG132, and higher than when MG132 was added only during the first or second 22 h of IVM. The progression of meiosis was arrested in prometaphase I or metaphase I when COCs were cultured for 44 h with MG132 or when the COCs were cultured for the first 22 h with MG132 (Fig. 4A). Interestingly, a majority of the ova treated with 100 μM MG132 failed to extrude first polar body and reach metaphase II, even if MG132 was present only during the second half of the IVM interval (Fig. 4A). Most oocytes cultured with 100 μM MG132 for 44 h (Fig. 4B) displayed intact nuclear envelopes with abundant NPCs and a high content of proteasomes similar to control GV-stage oocytes.

To examine whether the treatment with MG132 treatment could be used to extend the period of IVM, COCs were cultured in the presence of 10 μM MG132 for 44 h in TCM199 medium and then for 44 h under control IVM conditions (22 h in IVM medium with hormones followed by 22 h in medium without hormones). Despite doubling the time of in vitro culture, 50.1% of metaphase II oocytes were observed after 88 h of IVM (Supplemental Data Figure 2, available online at www.biolreprod.org).

Inhibition of Oocyte Meiosis by MG132 in Relation to Structural Integrity of TZP and Presence of Cumulus Cells

The above experiments did not address whether the inhibition of proteasomal activity by MG132 prevents GVBD

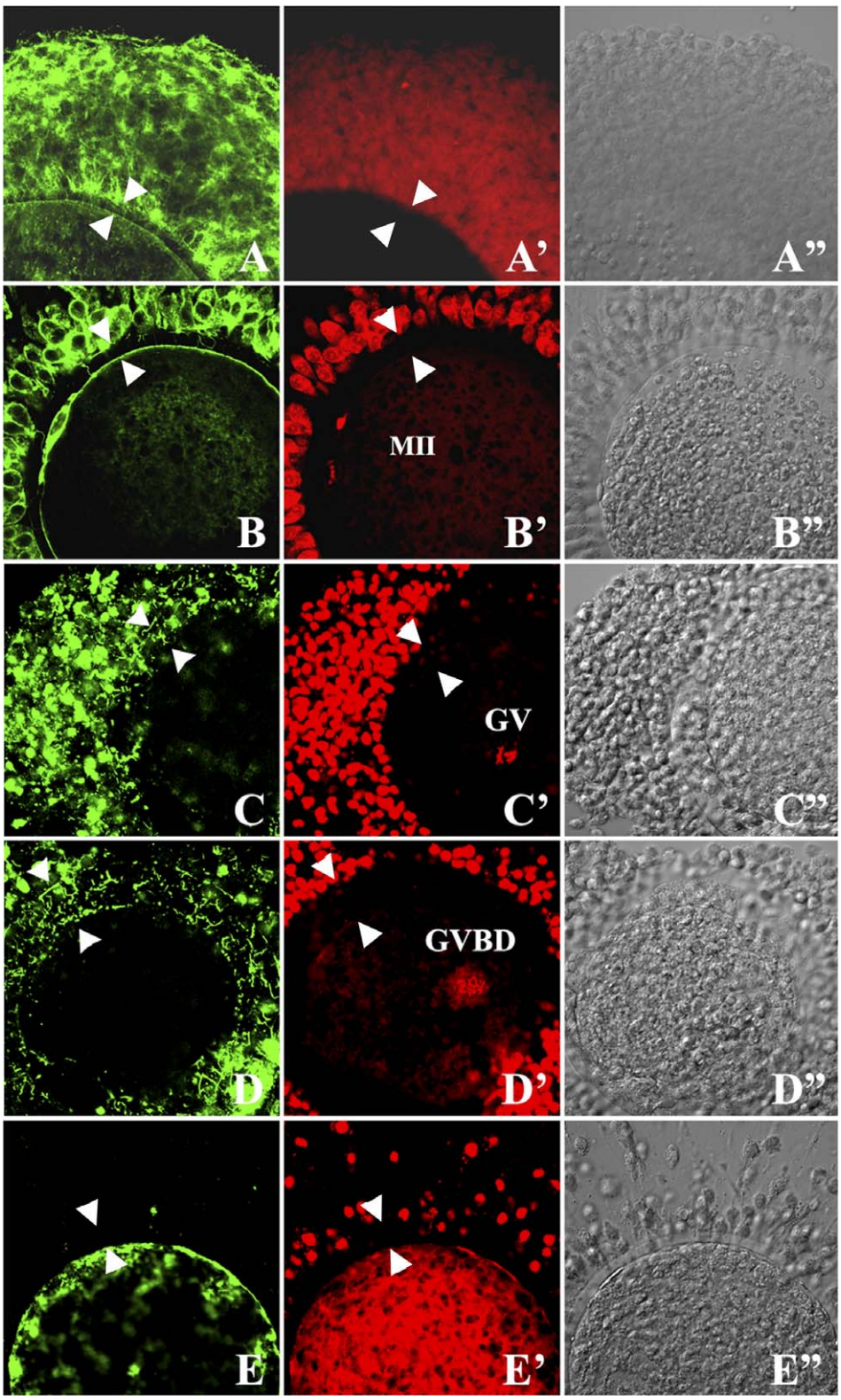

FIG. 1. Degradation of the transzonal projections (TZPs) in the porcine COCs matured in vitro under control conditions or in the presence of proteasomal inhibitor MG132 as visualized by laser scanning confocal microscopy. **A–A"**) Immature oocyte tightly surrounded by cumulus cells, with a diffuse distribution of microfilaments shown by Alexa Fluor 488-phalloidin. TZPs span zona pellucida (arrowheads) and reach the surface of the oocyte. **B–B"**) Few TZPs remain inside the zona pellucida after IVM. MII indicates metaphase II. **C–C"**) COCs cultured in the presence of MG132 in IVM medium for 44 h. Cumulus expansion was blocked by MG132, and the distribution of cumulus cells and TZPs (arrowheads) was similar to that of immature control COCs. GV indicates germinal vesicle. **D–D"**) COCs cultured in the presence of 10 μM MG132 in IVM medium for 22 h and then cultured without MG132 for 22 h. Few TZPs (arrowheads) still traverse the zona pellucida and reach the oocyte surface. Signs of cumulus expansion are present, including the assembly of microfilament bundles in cumulus cell cytoplasm. GVBD indicates germinal vesicle breakdown. **E–E"**) COCs cultured in the absence of MG132 in IVM medium for 22 h and then cultured with MG132 for 22 h. Cumuli oophori already expanded and few TZPs are present inside zona pellucida (arrowheads). Original magnification ×350.

directly by preventing the proteolysis of cell cycle-controlling proteins in the oocyte, or indirectly by blocking the destruction of TZP and cumulus-oocyte uncoupling. We devised a combined treatment with 10 μM MG132 and 10 μM CE, a microfilament disruptor that could induce actin microfilament depolymerization in the TZPs, leading to TZP breakdown independent of hormonal stimulation of COCs. First, we cultured the COCs in the presence or absence of CE the first 22 h of maturation in FSH/LH-supplemented medium, followed by 22 h of culture without hormones and with CE. These treatments did not significantly alter GVBD and the progression to metaphase I, whereas few ova reached metaphase II due to the cytochalasin-induced block of karyokinesis and cytokinesis (first polar body extrusion; Fig. 5A). While cumulus expansion was blocked by CE after 44 h of culture, the treatment coincided with the disruption of TZPs from ZP

and oocyte surface (Fig. 5B, a–a''). When the COCs were cultured in the presence of CE in IVM medium for 22 h and then cultured without CE for 22 h, the cumulus cells were connected loosely and few TZPs were present in the ZP (Fig. 5B, b–b''). In COCs cultured in the absence of CE for 22 h and then cultured with CE for next 22 h, the cumulus cells had already expanded within the first 22 h of culture, TZPs were disrupted, and weak staining of microfilaments was observed on the oocyte surface (Fig. 5B, c–c'') compared with the microfilament staining of TZPs and oocyte cortex in the control GV-stage oocytes (Fig. 5B, d–d'').

The combined treatment with 10 μM MG132 and 10 μM CE for 22 h did not inhibit the progression of meiosis up to metaphase I, a stage at which MG132 prevents the proteasomal degradation of cyclin B, a prelude to metaphase-anaphase transition [39]. Consequently, high rates of metaphase I (64.9%) ova were recorded, but the rates of GV stage ova (Fig. 5C) were similar to control, untreated, expanded COCs and COCs treated with CE alone. While cumulus expansion was blocked by the combination of MG132 and CE, the treatment with CE caused microfilament depolymerization and disruption of TZPs (Fig. 5D). Even though a low concentration of MG132 (10 μM) was not sufficient to maintain intact GV in the cumulus-enclosed ova, 90% of ova remained in GV stage when cumulus-free ova were subjected to 10 μM MG132 treatment for first 22 h of oocyte maturation (Fig. 5E). Thus, even a low concentration of MG132 prevented GVBD in the absence of cumulus cells.

MG132 Treatment Prevents the Synthesis and Deposition of Cumulus ECM

More than 90% of porcine COCs isolated from follicles 3 mm or larger undergo expansion during 24 h of culture in the presence of FSH [12]. In the present study, the presence of FSH/LH induced cumulus cells to expand within 24 h and synthesize HA (Fig. 6A). In the control FSH/LH-stimulated expanded complexes, the amount of HA retained within the complexes represented approximately 55% of the total amount of HA accumulated in the culture well (combined HA content of COCs and culture medium). Nevertheless, in the presence of FSH/LH and 100 μM MG132, all COCs remained compact, and total HA accumulation was reduced by 48% ($P < 0.001$; Fig. 6A). In addition, the retention of HA within the complexes decreased to <23% of the amount retained within the complexes cultured in the absence of MG132 ($P < 0.05$; Fig. 6A).

We next used immunoblotting with anti-IαI antibody to evaluate whether the heavy chains of serum-derived IαI-related molecules are covalently linked to HA in the presence of MG132, the covalent binding being required for ECM deposition. The nonexpanded control COCs (0 h; Fig. 6B) and COCs cultured for 22 h with MG132 (both digested with hyaluronidase) did not contain proteins reactive with IαI antibody. In contrast, matrix extracts of expanded COCs after culture without MG132 (22 h; Fig. 6B) or matrix extracts of in vivo-expanded COCs isolated from antral follicles of gilts treated sequentially with eCG and hCG (Fig. 6B), contained immunoreactive bands of approximately 120 kDa, 130 kDa, and 220 kDa. These respective bands were demonstrated recently in SDS-PAGE of porcine serum [32], and they correspond to IαI (bikunin plus HC1 and HC2), PαI (bikunin plus HC3), and IαLI (bikunin plus HC2), respectively [46, 47]. Two additional bands of approximately 75–85 kDa were detected in the matrix extracts of both types of COCs after digestion with hyaluronidase. Two other minor bands in the

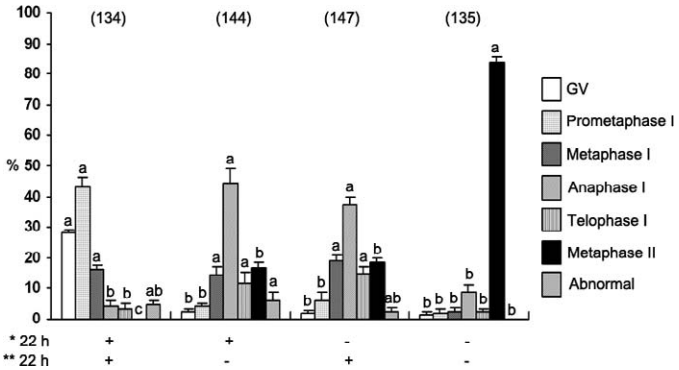

FIG. 2. Inhibitory effect of MG132 on the progression of oocyte meiosis. COCs were cultured in the presence or absence of 10 μM MG132 for the first *22 h of maturation in FSH/LH-supplemented medium, followed by **22 h of culture without hormones and with or without (+/–) 10 μM MG132. Experiments were repeated five times. Values are expressed as the mean percentage ± SEM. The numbers of cultured oocytes are indicated in parentheses. Different letters a, b, and c in each group of columns denote a significant difference at $P < 0.05$.

hyaluronidase matrix extract migrating at about 160–170 kDa likely represent dimers of the different types of heavy chains linked to the same HA strand at so close a proximity that the enzymatic digestion of the interposed HA fragment is prevented, as previously suggested by Chen et al. [29]. These observations confirm our previous results [32] that HCs from IαI-related molecules identified in the porcine serum were transferred and covalently linked to HA during porcine cumulus expansion in vivo and in vitro. However, cumulus expansion and the covalent transfer of HCs from IαI to HA were not observed in the presence of MG132 (Fig. 6). Immunoblotting with anti-actin antibody was used for normalization of IαI protein load.

MG132 Treatment Does Not Alter Microfilament Dynamics in Cumulus Cell Cytoplasm

The above data demonstrated that MG132 treatment prevented cumulus expansion and deposition of cumulus ECM. Apart from maintenance of F-actin-rich TZPs, MG132 treatment did not prevent microfilament dynamics within cumulus cell cytoplasm. We examined whether MG132 could affect the cumulus expansion by reducing the content of RAC1 GTPase, a major regulator of F-actin polymerization known to be turned over by UPP [48]. However, we observed neither major changes in RAC1 content in the course of cumulus expansion nor RAC1 accumulation in the presence of MG132 (Fig. 7). By epifluorescence microscopy, RAC1 colocalized with F-actin inside cumulus cells before and after cumulus expansion (Supplemental Data Figure 3, available online at www.biolreprod.org). Total content of β-actin (ACTB) was stable during cumulus expansion but increased in COCs matured in the presence of MG132 (Fig. 7B). In the same set of experiments, we also evaluated the cellular content of UCHL3. The UCHL3 and related deubiquitinating enzymes are believed to regulate the rate of proteasomal proteolysis [36]. Relative to ACTB expression, the content of UCHL3 was greatly diminished after 44 h of COC culture (Fig. 7A). This reduction of UCHL3 content seemed to occur during the last 12 h of culture and was not prevented by MG132 (Fig. 7B). It is possible that a feedback mechanism that signals the increased need for proteasomal degradation of proteins accumulating in the presence of a proteasomal core inhibitor also suppresses the

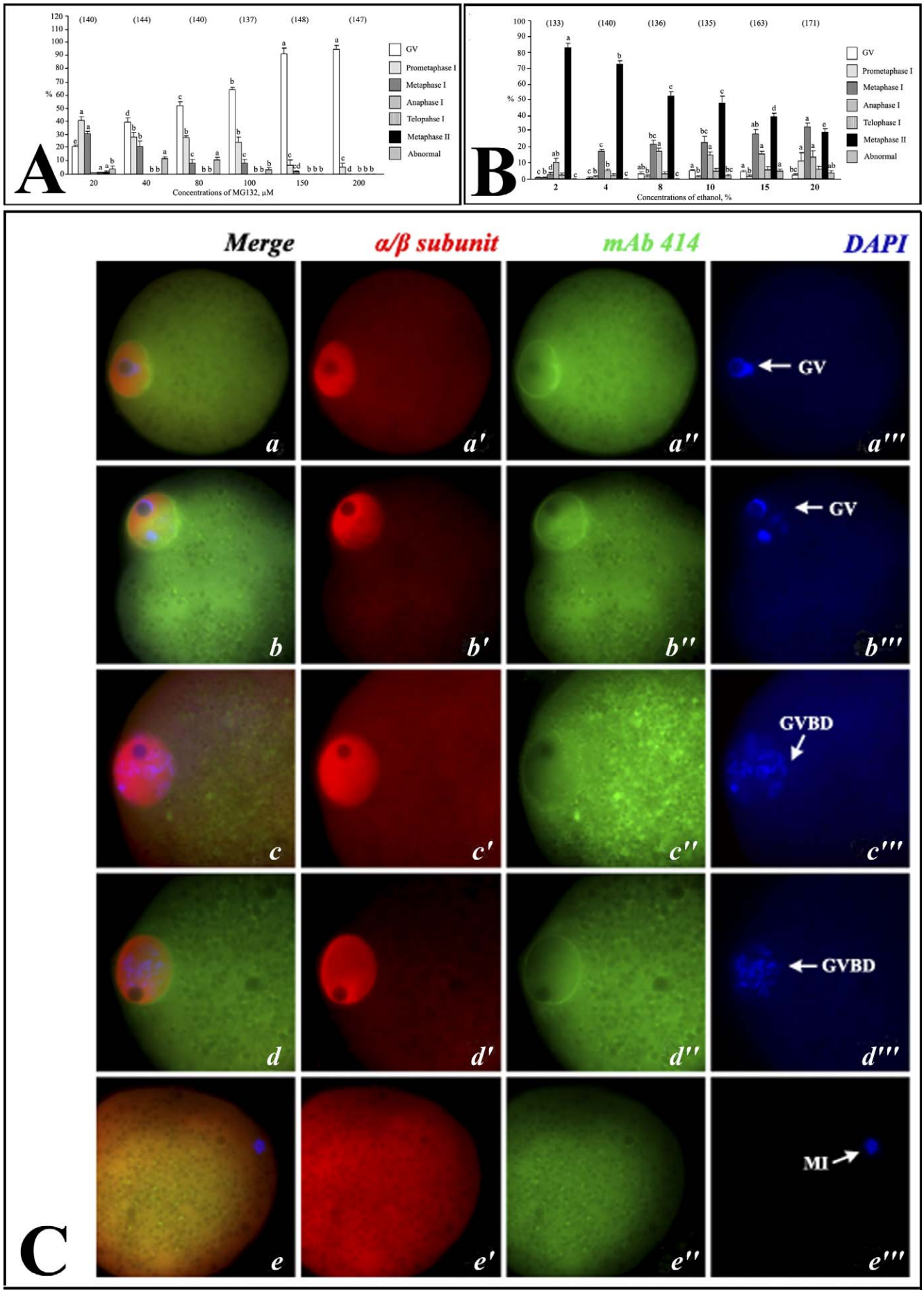

expression of deubiquitinating enzymes that could be limiting factors of proteasomal degradation.

DISCUSSION

The involvement of the UPP in oocyte maturation has been suggested previously in various species and taxa. However, the present study offers novel insight into mechanisms by which proteasomal proteolysis contributes to both the regulation of the oocyte cell cycle and to remodeling of its surrounding cumulus mass. In the present study, 10 μM MG132 maintained the percentage of GV-intact ova near 30% and the percentage of metaphase I oocytes above 40% in cumulus-enclosed porcine ova. However, when 10 μM MG132 was used in conjunction with 10 μM CE, an agent capable of disrupting TZPs of cumulus cells, the percentage of GV oocytes was reduced to 10%, and the percentage of metaphase I oocytes was increased proportionally, reaching ~70%. The arrest at metaphase I in both cases can be explained by the inhibitory effect of MG132 on proteasome-dependent cyclin degradation, preventing metaphase-anaphase transition [39, 43]. Our finding of low incidence of GV-intact oocytes in the presence of MG132 in conjunction with CE treatment suggests that the depolymerization of actin-rich TZPs by CE overruled the inhibitory effect of 10 μM MG132 on GVBD in the cumulus-enclosed ova. Metaphase-anaphase transition thus appears to be more sensitive to proteasomal inhibitors than GVBD. While high concentrations of MG132 (20–200 μM) prevented GVBD in a concentration-dependent manner, almost complete GV retention (>90%) was observed when cumulus-free ova were exposed to 10 μM MG132. Therefore, a higher level of proteasomal activity may be necessary to induce GVBD process in the absence of cumulus cell-produced, meiosis-stimulating factors. Possible substrates of UPP during GVBD could include cell cycle regulators, nuclear lamins, and histones. The inhibitory action of 10 μM MG132 on GVBD could be counteracted by the cumulus cell-produced, freely diffusible, meiosis-stimulating agents that may not require TZPs for their transport into ooplasm. At the same time, breakdown of TZPs with CE could stop the influx of meiosis-inhibiting substances through cumulus-to-oocyte gap junctions (GJs), explaining why MG132 at low concentrations was not sufficient to maintain intact GVs in presence of cumulus cells and CE. These observations suggest that the maintenance of TZPs supports oocyte meiotic arrest, possibly by the means of sustained high levels of cAMP. According to this hypothesis, cAMP is produced by the cumulus cells and transported to a meiotically quiescent oocyte via TZPs terminated by cumulus cell-to-oocyte GJs, permeant to cAMP [49]. In a recent study, carbonoxolone, a selective inhibitor of gap junctional communication, promoted meiotic maturation of follicle-enclosed rat oocytes in vitro and caused a significant decrease in intraoocyte concentration of cAMP [50]. Our thesis that the gonadotropin-

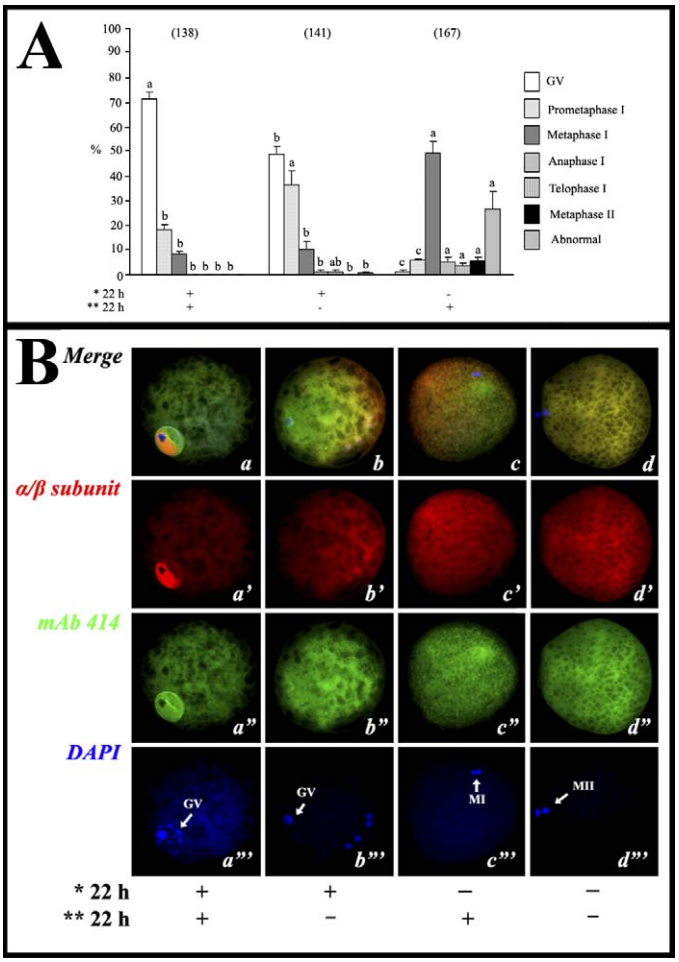

FIG. 4. Meiotic maturation, GV configurations, and the accumulation of proteasomes in porcine ova cultured in the presence of MG132 for up to 44 h as visualized by conventional epifluorescence microscopy. **A**) MG132 prevented GVBD when added during the first 22 h of maturation, but it had no effect on GVBD when added during second 22 h. COCs were cultured in the presence or absence of 100 μM MG132 for the first *22 h of maturation in FSH/LH-supplemented medium, followed by **22 h of culture without hormones and with or without (+/–) 100 μM MG132. Experiments were repeated five times. Values are expressed as the mean percentage ± SEM. The numbers of cultured oocytes are indicated in parentheses. Different letters a, b, and c in each group of columns denote a significant difference at $P < 0.05$. **B**) After maturation with or without 100 μM MG132, oocytes were processed with antibodies recognizing NPCs (green) and multiple α/β-type 20S proteasomal core subunits (red). DNA was stained with DAPI (blue). The NPCs and proteasomes were not detectable in treatment groups (**b**–**b‴**), (**c**–**c‴**) and (**d**–**d‴**) because of timely GVBD. However, when ova were cultured with 100 μM MG132 during the whole period of 44 h, intact NPCs and proteasomes were detected in their GVs (**a**–**a‴**). Arrows indicate GV, metaphase I (MI), and metaphase II (MII) stages, respectively (**a‴**, **b‴**, **c‴**, and **d‴**). Original magnification ×150.

FIG. 3. Effects of varied concentrations of proteasomal inhibitor MG132 on meiotic maturation of porcine ova in COCs matured in vitro, visualized by conventional epifluorescence microscopy. **A**) MG132 blocked GVBD and progression of meiosis in a dose-dependent manner. COCs were cultured with 20–200 μM MG132 in IVM medium for 44 h. **B**) Varied concentrations of ethanol (vehicle solution for MG132) corresponding to ethanol volume added to COCs with MG132 in **A** did not have a significant effect on meiotic maturation of porcine ova matured in vitro for 44 h. **A**, **B**) Experiments were repeated five times. Values are expressed as the mean percentage ± SEM. The numbers of cultured oocytes are indicated in parentheses. Different letters a, b, c, d, and e in each group of columns denote a significant difference at $P < 0.05$. **C**) Distribution of proteasomes (red, α-type and β-type subunits of the 20S core) and NPCs (green, labeled with mAb414) in porcine oocyte after first 22 h of IVM. Immature GV-stage oocytes (**a**–**a‴**) and oocytes from COCs cultured with 10 μM MG132 for 22 h in FSH/LH-supplemented medium (**b**–**b‴**) display 20S core subunit (red) in the GV. The GVBD was examined in the oocytes cultured with (**c**–**c‴**) or without (**d**–**d‴**) 10 μM MG132 for 22 h in FSH/LH-supplemented medium. The 20S proteasomal core subunits were detected inside the GV or around the condensing chromosomes after both treatments. However, the NPCs (green) disappeared progressively as the oocyte reached metaphase I (MI) during in vitro culture without MG132. The proteasomes became dissociated from oocyte chromatin as the oocytes reached metaphase I (**e**–**e‴**). DNA was counterstained with DAPI (blue). See Supplemental Data Figure 4 (available online at www.biolreprod.org), for negative control. Original magnification ×250.

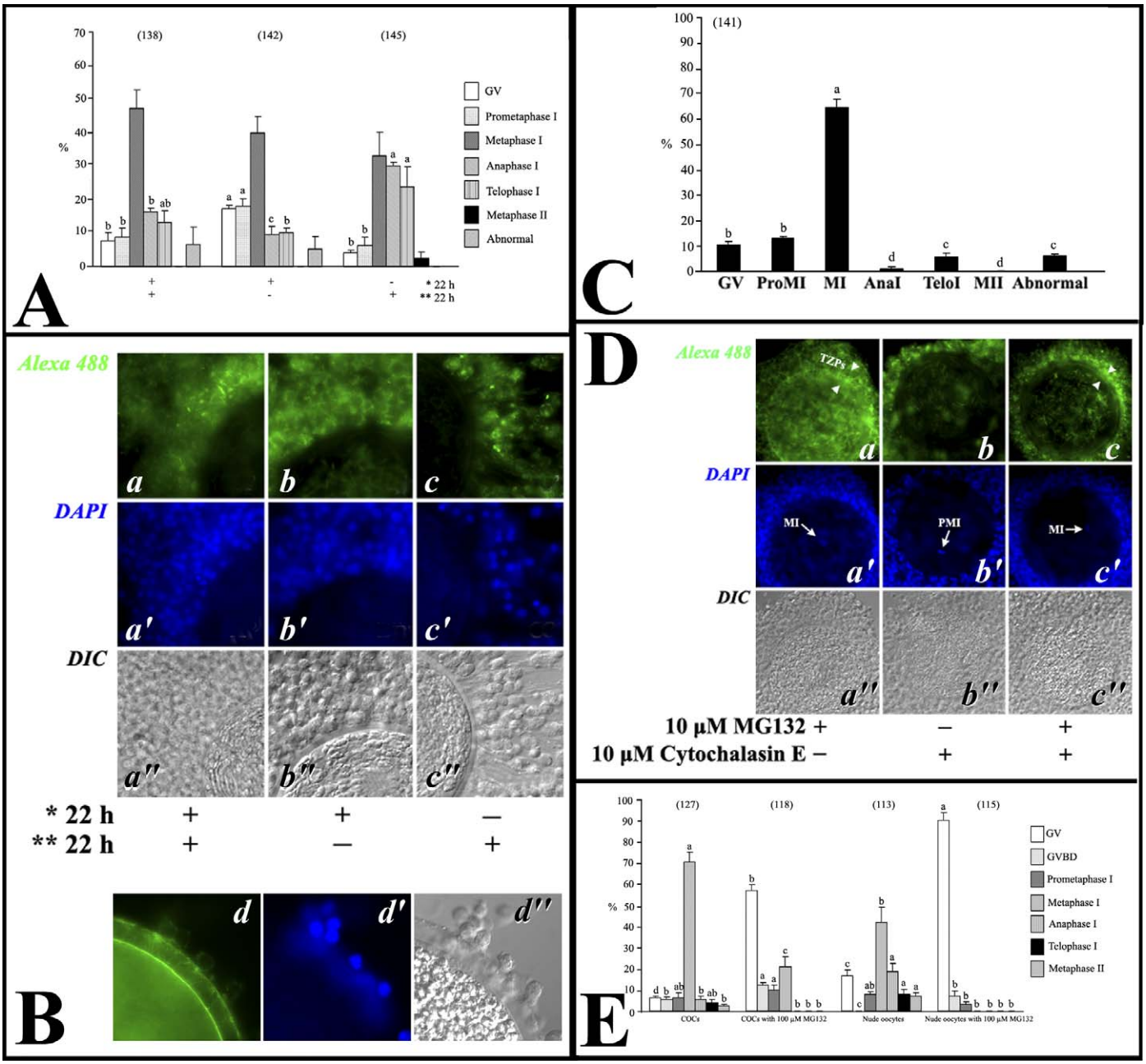

FIG. 5. Effect of combined treatment with MG132 and microfilament disruptor CE on porcine oocyte maturation and cumulus expansion. **A**) CE did not alter the progression of oocyte meiosis up to metaphase I. COCs were cultured in the presence or absence of 10 μM CE for the first *22 h of maturation in FSH/LH-supplemented medium, followed by **22 h of culture without hormones, with or without (+/–) 10 μM CE. Experiments were repeated five times. Values are expressed as the mean percentage ± SEM. The numbers of cultured oocytes are indicated in parentheses. Different letters a, b, and c in each group of columns denote a significant difference at $P < 0.05$. **B**) As shown by conventional epifluorescence microscopy, CE induced the breakdown of TZPs but prevented cumulus expansion. **a**–**a"**) Cumulus expansion was blocked by CE, and TZPs disappeared from the zona pellucida and oocyte surface in COCs cultured with CE for the whole 44 h of IVM. **b**–**b"**) Absence of TZPs in the COCs cultured in the presence of CE in IVM medium for 22 h and then cultured without CE for 22 h. **c**–**c"**) No TZPs were present in the zona pellucida in COCs cultured in the absence of CE in IVM medium for 22 h and then cultured with CE for 22 h. Cumulus cells already expanded under the influence of gonadotropins and TZPs disappeared from the zona pellucida and oocyte surface. **d**–**d''**) Microfilament staining of TZPs and oocyte cortex in the control GV-stage oocytes. Original magnification ×200 (**a**–**c"**) and ×300 (**d**–**d"**). **C**) Effect of CE superseded the effect of MG132 in a combined treatment during in vitro culture of COCs. Rates of GVBD in the combined treatment with MG132 and CE were similar to control COCs (compare with Fig. 2) and those treated with CE alone (compare with Fig. 5A). COCs were cultured with a combination of 10 μM MG132 and 10 μM CE for 44 h. Meiotic maturation was examined after 44 h of IVM by DAPI staining. ProMI, prometaphase I; MI, metaphase I; AnaI, anaphase I; TeloI, telophase I; MII, metaphase II. Experiments were repeated five times. Values are expressed as the mean percentage ± SE. The numbers of cultured oocytes are indicated in parentheses. Different letters a, b, c, and d denote a significant difference at $P < 0.05$. **D**) Cotreatment with CE reversed the MG132-induced block of TZP breakdown. **a**–**a''**) COCs were cultured with 10 μM MG132 for 44 h. Cumulus expansion was blocked, and the intact TZPs (arrowheads) were present in zona pellucida. The oocyte chromosomes were at metaphase I stage (MI; arrow). **b**–**b''**) COCs were cultured with 10 μM CE for 44 h. Cumulus expansion was blocked, and TZPs disappeared from the zona pellucida and oocyte surface. The oocyte chromosomes were at prometaphase I (PMI; arrow) stage. **c**–**c''**) COCs were cultured with a combination of 10 μM MG132 and 10 μM CE for 44 h. Cumulus expansion was blocked, and few TZPs (arrowheads) were present in the zona pellucida. The oocyte chromosomes were at metaphase I (MI; arrow) stage. All images were taken by a conventional epifluorescence microscope. Original magnification ×100. **E**) COCs and denuded oocytes (removed cumulus cells) were cultured in the presence or absence of 100 μM MG132 for 22 h in IVM medium with hormones. Experiments were repeated five times. Values are expressed as the mean percentage ± SE. The numbers of cultured oocytes are indicated in parentheses. Different letters a, b, c, and d in each group of columns denote a significant difference at $P < 0.05$.

induced breakdown of TZPs depends upon proteasomal degradation is further supported by the observation that MG132 alone sufficiently protected TZPs from breakdown in the presence of gonadotropins. Consequently, the maintenance of TZPs in the presence of MG132 reduced the rate of GVBD, and this MG132-induced inhibition was cancelled by microfilament depolymerization with CE. Traditionally, the uncoupling of cumulus-to-oocyte communication at the onset of oocyte maturation has been interpreted as the withdrawal of TZPs from zona pellucida [51, 52]. Our data suggest that this process may involve regulated, substrate-specific proteasomal proteolysis of proteins associated with actin microfilaments within TZPs. For example, ubiquitination and proteasomal degradation of actin-associated RAC1 GTPase occurs during early stages of epithelial cell scattering, an event that requires microfilament depolymerization in focal adhesions [48]. In our studies, the levels of RAC1 appeared relatively stable during cumulus expansion, and F-actin was observed with and without MG132. This observation alone does not rule out that a small subset of RAC1 molecules associated with TZPs could be degraded locally at the time of meiotic resumption. While MG132 did not cause accumulation of RAC1, it did induce a substantial increase in content of total ACTB (monomeric and F-actin). It is possible that actin in the TZPs is directly ubiquitinated and degraded by proteasomes during meiotic maturation. Ubiquitination and proteasomal degradation of actin and actin-associated proteins has been suggested as a possible cause of skeletal muscle atrophy [53]. While high levels of RAC1 may be important for the sustenance of cumulus mass before and during expansion, degradation of UCHL3, which is an important rate-limiting factor of proteasomal proteolysis, may reflect an increased need for proteasomal proteolysis during cumulus expansion.

The exact function of the 26S proteasome in cumulus expansion remains to be elucidated. In the present study, proteasomal inhibitor MG132 prevented cumulus expansion, and cumulus cells remained packed around the oocytes after 44 h of culture in a gonadotropin-supplemented medium. During preovulatory cumulus expansion, cumulus cells synthesize a large amount of HA that is organized in a highly hydrated, mucoelastic matrix. Figure 6 shows that 100 μM MG132 affected the organization of cumulus ECM and prevented HC translocation to HA in the COCs stimulated with gonadotropins. Furthermore, the FSH/LH-stimulated synthesis of HA was significantly reduced by MG132. Lower concentrations of MG132 (e.g., 10 μM; data not shown) did not reduce HA synthesis measured as total synthesis, but they significantly reduced the retention of synthesized HA within the COCs and still prevented cumulus expansion. In addition to HA synthesis, serum components belonging to the IαI family play a key role in porcine cumulus ECM deposition [32]. The formation of HA-enriched cumulus ECM is not supported by IαI-immunodepleted serum while it occurs in the presence of purified IαI molecules [27]. In the present study, the effect of MG132 on covalent linkage of heavy chains of IαI to HA, critical for cross-linking of HA strands and stabilization of cumulus matrix, was studied. Our Western blotting results clearly demonstrate that heavy chains of serum-derived IαI-related molecules become covalently linked to HA in pig COCs expanded in vitro only in the absence of MG132. This observation indicates that proteasomal proteolysis is essential for cumulus expansion and assembly of cumulus ECM. To our knowledge, this is the first demonstration of the requirement of proteasomal proteolysis during the process of cumulus expansion.

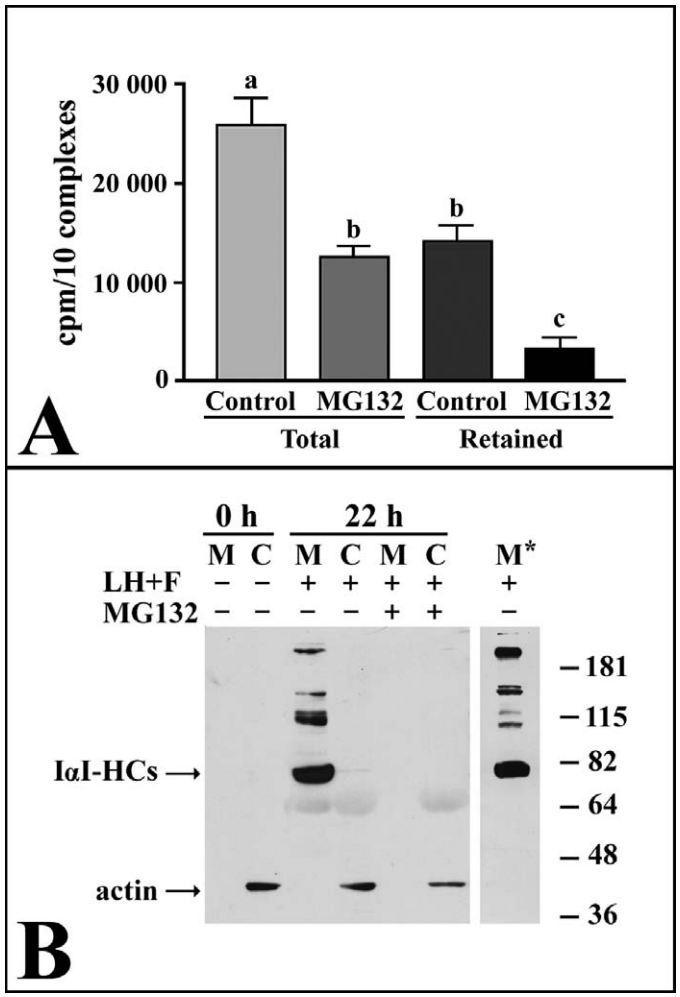

FIG. 6. Proteasomal proteolysis is required for the synthesis and deposition of cumulus ECM during IVM of porcine COCs. **A**) Effect of MG132 on synthesis of HA. Total (culture medium plus COCs) and retained HA (within COCs alone, obtained by repeated washing of the complexes after culture period) synthesized by FSH/LH stimulated COCs during 23 h of culture in medium containing 100 μM or no MG132 (control). Data represent the mean percentage ± SEM from three replicates, for a total of 30 COCs per treatment. Bars with different letters are significantly different. **B**) Detection of IαI in COCs cultured in vitro with and without MG132. Groups of 30 COCs were collected before (0 h) and after (22 h) in vitro culture in the presence of FSH/LH with or without 100 μM MG132. Lanes M and C represent matrix and cell pellet extracts (released by hyaluronidase treatment), respectively. Matrix (M*) extract represents three in vivo-expanded COCs isolated from eCG-primed pigs 24 h after hCG injection (digested with hyaluronidase) and used for comparison. Anti-actin antibody was used as a loading control for normalization of total protein content per lane. Representative autoradiographs are shown; two independent repeats were performed with similar results.

The results of a combined treatment with MG132 and CE suggest that cytoskeletal reorganization precedes ECM deposition in the signaling cascade of cumulus expansion. A similar phenomenon was observed when COCs were cultured with progesterone receptor (PR) antagonist RU486. Cumulus cells of COCs treated with RU486 remained tightly packed around the oocytes, with little visible expansion [54]. Other proteases besides 26S proteasome could also be involved in the reorganization of cumulus ECM during cumulus expansion. ADAMTS-1, a member of the disintegrin and metaloproteinase family of proteases, has been shown to degrade members of the lectican family of proteoglycans [55–57]. Production of

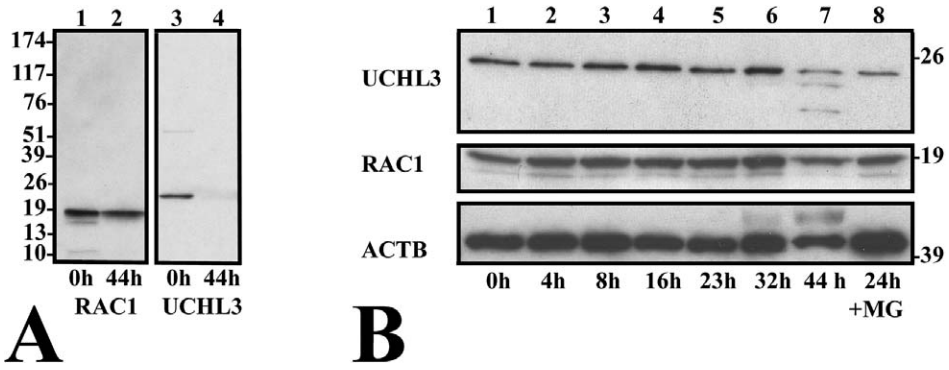

FIG. 7. Cellular content of RAC1 GTPase (RAC1; modulator of actin-polymerization turned over by UPP) and UCHL3 (deubiquitinating enzyme with rate-limiting activity toward 26 S proteasome) in the cumulus cells during porcine oocyte maturation. **A**) Comparison of RAC1 and UCHL3 content before and after cumulus expansion. RAC1 blot was stripped and reprobed with anti-UCHL3 (30 COCs per lane). **B**) Time-lapse Western blot of RAC1, UCHL3, and β-actin (ACTB) during 44 h of in vitro culture with gonadotropins (lanes 1–7) and in COCs cultured for 44 h with gonadotropins and MG132 (lane 8). Thirty COCs per lane were loaded. RAC1 levels were stable during cumulus expansion with or without MG132, favoring uninterrupted F-actin polymerization. UCHL3 levels declined toward the end of culture period, despite MG132 treatment. Actin levels were relatively stable, but they increased substantially in the presence of MG132.

ADAMTS-1 protein is induced by LH in granulosa cells via progesterone- and PR-dependent pathways [58–60] and cleaves versican (VI variant) in human aorta in vivo, releasing a 70-kDa N-terminal fragment [61]. In the expanded COCs, a 70-kDa N-terminal VI fragment appears to be generated by an ADAMTS-1 proteaselike activity [60]. Since the cleaved N-terminal domain of versican binds the HA-rich matrix, the cleaved versican may serve to stabilize cumulus expansion of COC. The ADAMTS-1 mRNA in cumulus cells of COCs is dramatically upregulated in response to gonadotropins [54] and downregulated by RU486. While the cumulus expansion is compromised in the RU486-treated COCs, the treated cumulus cells still show patterns of HAS-2, TNFAIP6, versican, and ADAMTS-4 expression similar to those of control, expanded COCs [54]. This result is reminiscent of apparently normal cumulus HA synthesis in the presence of expansion-blocking 10 μM MG132 in our study.

Proteasomes may also participate in protein turnover inside the cells of expanding COCs. One example is the ubiquitin-proteasome dependent turnover of steroidogenic acute regulatory protein (STAR) in granulosa cells. STAR is synthesized as a 37-kDa preprotein in the cytoplasm of steroidogenic cells and is then rapidly transported into mitochondria, where it is cleaved, generating 32-kDa and 30-kDa proteins [62, 63]. STAR plays a key role in rapid modulation of steroidogenesis in the ovary [64] and testis [65]. Rat granulosa cells and immortalized human granulosa cells treated with MG132 accumulate STAR [66]. The MG132-induced STAR accumulation is further augmented in the presence of forskolin, LH, or FSH [66]. The cytosolic 37-kDa STAR preprotein, which is responsible for the steroidogenic activity of STAR, is the primary proteasomal substrate, and the inhibition of its degradation by MG132 causes the upregulation of progesterone production [66]. Proteasomal activity may also be important for quality control during the synthesis and secretion of ECM glycoprotein by cumulus cells. Ubiquitination and proteasomal degradation of improperly glycosylated, unassembled, and misfolded glycoproteins is a central element of the endoplasmic reticulum-associated ERAD system for protein quality control in the secretory pathway [67]. Accumulation of aberrant, misfolded ECM proteins in the presence of MG132 could prevent their interactions with HA after secretion.

Together, our data suggest that proteasomal activity has multiple functions in oocyte meiosis, in cumulus expansion, in the synthesis and processing of cumulus ECM, and in the modification of cumulus-oocyte communication. Maintenance of TZPs of cumulus cells may be required for the maintenance of meiotic arrest in the cumulus-enclosed oocytes, and the gonadotropin-induced proteasomal degradation of cytoskeletal proteins in these projections may contribute to resumption of oocyte meiosis. In the ooplasm, proteasomal activity is required for metaphase-anaphase transition, as shown previously in mammals, but also for the process of GVBD.

ACKNOWLEDGMENTS

We thank Nicole Leitman for technical support, the laboratory of Dr. Randall Prather for collecting porcine ovaries, and Kathryn Craighead for clerical support and manuscript editing.

REFERENCES

1. Tanghe S, Van Soom A, Nauwynck H, Coryn M, de Kruif A. Minireview: functions of the cumulus oophorus during oocyte maturation, ovulation, and fertilization. Mol Reprod Dev 2002; 61:414–424.
2. Chun SY, Eisenhauer KM, Minami S, Billig H, Perlas E, Hsueh AJ. Hormonal regulation of apoptosis in early antral follicles: follicle-stimulating hormone as a major survival factor. Endocrinology 1996; 137:1447–1456.
3. Chen L, Wert SE, Hendrix EM, Russell PT, Cannon M, Larsen WJ. Hyaluronic acid synthesis and gap junction endocytosis are necessary for normal expansion of the cumulus mass. Mol Reprod Dev 1990; 26:236–247.
4. Sutovsky P, Flechon JE, Flechon B, Motlik J, Peynot N, Chesne P, Heyman Y. Dynamic changes of gap junctions and cytoskeleton during in vitro culture of cattle oocyte cumulus complexes. Biol Reprod 1993; 49: 1277–1287.
5. Eppig JJ. FSH stimulates hyaluronic acid synthesis by oocyte-cumulus cell complexes from mouse preovulatory follicles. Nature 1979; 281:483–484.
6. Eppig JJ. Gonadotropin stimulation of the expansion of cumulus oophori isolated from mice: general conditions for expansion in vitro. J Exp Zool 1979; 208:111–120.
7. Buccione R, Vanderhyden BC, Caron PJ, Eppig JJ. FSH-induced expansion of the mouse cumulus oophorus in vitro is dependent upon a specific factor(s) secreted by the oocyte. Dev Biol 1990; 138:16–25.
8. Shimada M. The gonadotropin-induced cumulus cell differentiations play important roles in in vitro meiotic maturation of porcine oocytes. In: Tokumoto T (ed.), New Impact on Protein Modifications in the Regulation of Reproductive System. Kerala, India: Research Signpost; 2005:1–18.
9. Salustri A, Yanagishita M, Hascall VC. Synthesis and accumulation of hyaluronic acid and proteoglycans in the mouse cumulus cell-oocyte complex during follicle-stimulating hormone-induced mucification. J Biol Chem 1989; 264:13840–13847.
10. Allworth AE, Albertini DF. Meiotic maturation in cultured bovine oocytes

is accompanied by remodeling of the cumulus cell cytoskeleton. Dev Biol 1993; 158:101–112.
11. Sutovsky P, Flechon JE, Pavlok A. F-actin is involved in control of bovine cumulus expansion. Mol Reprod Dev 1995; 41:521–529.
12. Prochazka R, Srsen V, Nagyova E, Miyano T, Flechon JE. Developmental regulation of effect of epidermal growth factor on porcine oocyte-cumulus cell complexes: nuclear maturation, expansion, and F-actin remodeling. Mol Reprod Dev 2000; 56:63–73.
13. Motta PM, Makabe S, Naguro T, Correr S. Oocyte follicle cells association during development of human ovarian follicle. A study by high resolution scanning and transmission electron microscopy. Arch Histol Cytol 1994; 57:369–394.
14. Dekel N, Hillensjo T, Kraicer PF. Maturational effects of gonadotropins on the cumulus-oocyte complex of the rat. Biol Reprod 1979; 20:191–197.
15. Eppig JJ. Regulation of cumulus oophorus expansion by gonadotropins in vivo and in vitro. Biol Reprod 1980; 23:545–552.
16. Eppig JJ. Role of serum in FSH stimulated cumulus expansion by mouse oocyte-cumulus cell complexes in vitro. Biol Reprod 1980; 22:629–633.
17. Motlik J, Fulka J, Flechon JE. Changes in intercellular coupling between pig oocytes and cumulus cells during maturation in vivo and in vitro. J Reprod Fertil 1986; 76:31–37.
18. Prochazka R, Nagyova E, Rimkevicova Z, Nagai T, Kikuchi K, Motlik J. Lack of effect of oocytectomy on expansion of the porcine cumulus. J Reprod Fertil 1991; 93:569–576.
19. Thibault C, Szollosi D, Gerard M. Mammalian oocyte maturation. Reprod Nutr Dev 1987; 27:865–896.
20. Dekel N, Kraicer PF. Induction in vitro of mucification of rat cumulus oophorus by gonadotrophins and adenosine 3′,5′-monophosphate. Endocrinology 1978; 102:1797–1802.
21. Fukui Y, Sakuma Y. Maturation of bovine oocytes cultured in vitro: relation to ovarian activity, follicular size and the presence or absence of cumulus cells. Biol Reprod 1980; 22:669–673.
22. Chian RC, Niwa K, Sirard MA. Effects of cumulus cells on male pronuclear formation and subsequent early development of bovine oocytes in vitro. Theriogenology 1994; 41:1499–1508.
23. Eppig JJ, Ward-Bailey PF. Sulfated glycosaminoglycans inhibit hyaluronic acid synthesizing activity in mouse cumuli oophori. Exp Cell Res 1984; 150:459–465.
24. Salustri A, Yanagishita M, Hascall VC. Mouse oocytes regulate hyaluronic acid synthesis and mucification by FSH-stimulated cumulus cells. Dev Biol 1990; 138:26–32.
25. Salustri A, Yanagishita M, Underhill CB, Laurent TC, Hascall VC. Localization and synthesis of hyaluronic acid in the cumulus cells and mural granulosa cells of the preovulatory follicle. Dev Biol 1992; 151: 541–551.
26. Nagyova E, Prochazka R, Vanderhyden BC. Oocytectomy does not influence synthesis of hyaluronic acid by pig cumulus cells: retention of hyaluronic acid after insulin-like growth factor-I treatment in serum-free medium. Biol Reprod 1999; 61:569–574.
27. Chen L, Mao SJ, Larsen WJ. Identification of a factor in fetal bovine serum that stabilizes the cumulus extracellular matrix. A role for a member of the inter-alpha-trypsin inhibitor family. J Biol Chem 1992; 267:12380–12386.
28. Zhuo L, Yoneda M, Zhao M, Yingsung W, Yoshida N, Kitagawa Y, Kawamura K, Suzuki T, Kimata K. Defect in SHAP-hyaluronan complex causes severe female infertility. A study by inactivation of the bikunin gene in mice. J Biol Chem 2001; 276:7693–7696.
29. Chen L, Zhang H, Powers RW, Russell PT, Larsen WJ. Covalent linkage between proteins of the inter-alpha-inhibitor family and hyaluronic acid is mediated by a factor produced by granulosa cells. J Biol Chem 1996; 271: 19409–19414.
30. Odum L, Andersen CY, Jessen TE. Characterization of the coupling activity for the binding of inter-alpha-trypsin inhibitor to hyaluronan in human and bovine follicular fluid. Reproduction 2002; 124:249–257.
31. Fulop C, Szanto S, Mukhopadhyay D, Bardos T, Kamath RV, Rugg MS, Day AJ, Salustri A, Hascall VC, Glant TT, Mikecz K. Impaired cumulus mucification and female sterility in tumor necrosis factor-induced protein-6 deficient mice. Development 2003; 130:2253–2261.
32. Nagyova E, Camaioni A, Prochazka R, Salustri A. Covalent transfer of heavy chains of inter-alpha-trypsin inhibitor family proteins to hyaluronan in in vivo and in vitro expanded porcine oocyte-cumulus complexes. Biol Reprod 2004; 71:1838–1843.
33. Hershko A, Ciechanover A. The ubiquitin system. Annu Rev Biochem 1998; 67:425–479.
34. Voges D, Zwickl P, Baumeister W. The 26S proteasome: a molecular machine designed for controlled proteolysis. Annu Rev Biochem 1999; 68:1015–1068.
35. Groll M, Ditzel L, Lowe J, Stock D, Bochtler M, Bartunik HD, Huber R. Structure of 20S proteasome from yeast at 2.4 A resolution. Nature 1997; 386:463–471.
36. Guterman A, Glickman MH. Deubiquitinating enzymes are IN/(trinsic to proteasome function). Curr Protein Pept Sci 2004; 5:201–211.
37. Tokumoto T. Nature and role of proteasomes in maturation of fish oocytes. Int Rev Cytol 1999; 186:261–294.
38. Takagi Sawada M, Kyozuka K, Morinaga C, Izumi K, Sawada H. The proteasome is an essential mediator of the activation of pre-MPF during starfish oocyte maturation. Biochem Biophys Res Commun 1997; 236:40–43.
39. Josefsberg LB, Galiani D, Dantes A, Amsterdam A, Dekel N. The proteasome is involved in the first metaphase-to-anaphase transition of meiosis in rat oocytes. Biol Reprod 2000; 62:1270–1277.
40. Chmelikova E, Sedmikova M, Rajmon R, Petr J, Svestkova D, Jilek F. Effect of proteasome inhibitor MG132 on in vitro maturation of pig oocytes. Zygote 2004; 12:157–162.
41. Huo LJ, Fan HY, Zhong ZS, Chen DY, Schatten H, Sun QY. Ubiquitin-proteasome pathway modulates mouse oocyte meiotic maturation and fertilization via regulation of MAPK cascade and cyclin B1 degradation. Mech Dev 2004; 121:1275–1287.
42. Tan X, Peng A, Wang Y, Tang Z. The effects of proteasome inhibitor lactacystin on mouse oocyte meiosis and first cleavage. Sci China C Life Sci 2005; 48:287–294.
43. Glotzer M, Murray AW, Kirschner MW. Cyclin is degraded by the ubiquitin pathway. Nature 1991; 349:132–138.
44. Abeydeera LR, Wang WH, Prather RS, Day BN. Maturation in vitro of pig oocytes in protein-free culture media: fertilization and subsequent embryo development in vitro. Biol Reprod 1998; 58:1316–1320.
45. Sutovsky P. Visualization of sperm accessory structures in the mammalian spermatids, spermatozoa, and zygotes by immunofluorescence, confocal, and immunoelectron microscopy. Methods Mol Biol 2004; 253:59–77.
46. Rouet P, Raguenez G, Tronche F, Yaniv M, N'Guyen C, Salier JP. A potent enhancer made of clustered liver-specific elements in the transcription control sequences of human alpha 1-microglobulin/bikunin gene. J Biol Chem 1992; 267:20765–20773.
47. Carrette O, Mizon C, Sautiere P, Sesboue R, Mizon J. Purification and characterization of pig inter-alpha-inhibitor and its constitutive heavy chains. Biochim Biophys Acta 1997; 1338:21–30.
48. Lynch EA, Stall J, Schmidt G, Chavrier P, D'Souza-Schorey C. Proteasome-mediated degradation of Rac1-GTP during epithelial cell scattering. Mol Biol Cell 2006; 17:2236–2242.
49. Dekel N, Lawrence TS, Gilula NB, Beers WH. Modulation of cell-to-cell communication in the cumulus-oocyte complex and the regulation of oocyte maturation by LH. Dev Biol 1981; 86:356–362.
50. Sela-Abramovich S, Edry I, Galiani D, Nevo N, Dekel N. Disruption of gap junctional communication within the ovarian follicle induces oocyte maturation. Endocrinology 2006; 147:2280–2286.
51. Hyttel P. Bovine cumulus-oocyte disconnection in vitro. Anat Embryol (Berl) 1987; 176:41–44.
52. Combelles CM, Albertini DF, Racowsky C. Distinct microtubule and chromatin characteristics of human oocytes after failed in-vivo and in-vitro meiotic maturation. Hum Reprod 2003; 18:2124–2130.
53. Ventadour S, Attaix D. Mechanisms of skeletal muscle atrophy. Curr Opin Rheumatol 2006; 18:631–635.
54. Shimada M, Nishibori M, Yamashita Y, Ito J, Mori T, Richards JS. Down-regulated expression of A disintegrin and metalloproteinase with thrombospondin-like repeats-1 by progesterone receptor antagonist is associated with impaired expansion of porcine cumulus-oocyte complexes. Endocrinology 2004; 145:4603–4614.
55. Kuno K, Iizasa H, Ohno S, Matsushima K. The exon/intron organization and chromosomal mapping of the mouse ADAMTS-1 gene encoding an ADAM family protein with TSP motifs. Genomics 1997; 46:466–471.
56. Kuno K, Kanada N, Nakashima E, Fujiki F, Ichimura F, Matsushima K. Molecular cloning of a gene encoding a new type of metalloproteinase-disintegrin family protein with thrombospondin motifs as an inflammation associated gene. J Biol Chem 1997; 272:556–562.
57. Kuno K, Matsushima K. ADAMTS-1 protein anchors at the extracellular matrix through the thrombospondin type I motifs and its spacing region. J Biol Chem 1998; 273:13912–13917.
58. Espey LL, Yoshioka S, Russell DL, Robker RL, Fujii S, Richards JS. Ovarian expression of a disintegrin and metalloproteinase with thrombospondin motifs during ovulation in the gonadotropin-primed immature rat. Biol Reprod 2000; 62:1090–1095.
59. Robker RL, Russell DL, Espey LL, Lydon JP, O'Malley BW, Richards JS. Progesterone-regulated genes in the ovulation process: ADAMTS-1 and cathepsin L proteases. Proc Natl Acad Sci U S A 2000; 97:4689–4694.

60. Russell DL, Doyle KM, Ochsner SA, Sandy JD, Richards JS. Processing and localization of ADAMTS-1 and proteolytic cleavage of versican during cumulus matrix expansion and ovulation. J Biol Chem 2003; 278: 42330–42339.
61. Sandy JD, Westling J, Kenagy RD, Iruela-Arispe ML, Verscharen C, Rodriguez-Mazaneque JC, Zimmermann DR, Lemire JM, Fischer JW, Wight TN, Clowes AW. Versican V1 proteolysis in human aorta in vivo occurs at the Glu441-Ala442 bond, a site that is cleaved by recombinant ADAMTS-1 and ADAMTS-4. J Biol Chem 2001; 276:13372–13378.
62. Stocco DM, Clark BJ. Regulation of the acute production of steroids in steroidogenic cells. Endocr Rev 1996; 17:221–244.
63. Strauss JF III, Kallen CB, Christenson LK, Watari H, Devoto L, Arakane F, Kiriakidou M, Sugawara T. The steroidogenic acute regulatory protein (StAR): a window into the complexities of intracellular cholesterol trafficking. Recent Prog Horm Res 1999; 54:369–394; discussion 394–365.
64. Sugawara T, Holt JA, Driscoll D, Strauss JF III, Lin D, Miller WL, Patterson D, Clancy KP, Hart IM, Clark BJ, Stocco DM. Human steroidogenic acute regulatory protein: functional activity in COS-1 cells, tissue-specific expression, and mapping of the structural gene to 8p11.2 and a pseudogene to chromosome 13. Proc Natl Acad Sci U S A 1995; 92: 4778–4782.
65. Gradi A, Tang-Wai R, McBride HM, Chu LL, Shore GC, Pelletier J. The human steroidogenic acute regulatory (StAR) gene is expressed in the urogenital system and encodes a mitochondrial polypeptide. Biochim Biophys Acta 1995; 1258:228–233.
66. Tajima K, Babich S, Yoshida Y, Dantes A, Strauss JF III, Amsterdam A. The proteasome inhibitor MG132 promotes accumulation of the steroidogenic acute regulatory protein (StAR) and steroidogenesis. FEBS Lett 2001; 490:59–64.
67. Meusser B, Hirsch C, Jarosch E, Sommer T. ERAD: the long road to destruction. Nat Cell Biol 2005; 7:766–772.